

# Bidirectional causal inference for binary outcomes in the presence of unmeasured confounding

Yafang Deng<sup>1</sup>, Kang Shuai<sup>2</sup>, Shanshan Luo<sup>1</sup>

<sup>1</sup> School of Mathematics and Statistics,  
Beijing Technology and Business University

<sup>2</sup> The Dartmouth Institute for Health Policy and Clinical Practice,  
Geisel School of Medicine at Dartmouth

## Abstract

Bidirectional causal relationships arising from mutual interactions between variables are commonly observed within biomedical, econometrical, and social science contexts. When such relationships are further complicated by unobserved factors, identifying causal effects in both directions becomes especially challenging. For continuous variables, methods that utilize two instrumental variables from both directions have been proposed to explore bidirectional causal effects in linear models. However, the existing techniques are not applicable when the key variables of interest are binary. To address these issues, we propose a structural equation modeling approach that links observed binary variables to continuous latent variables through a constrained mapping. We further establish identification results for bidirectional causal effects using a pair of instrumental variables. Additionally, we develop an estimation method for the corresponding causal parameters. We also conduct sensitivity analysis under scenarios where certain identification conditions are violated. Finally, we apply our approach to investigate the bidirectional causal relationship between heart disease and diabetes, demonstrating its practical utility in biomedical research.

**Keywords:** Bidirectional causal inference; Binary outcomes; Instrumental variables; Selection mechanism; Sensitivity analysis.

## 1 Introduction

The emergence of feedback mechanisms between entities often signifies mutual causal influences, a ubiquitous phenomenon across real-world systems (Engelgau et al., 2019; Riaz et al., 2017; Smith, 1999). In economics, a bidirectional causal relationship exists between health status and wealth accumulation: poor health erodes economic resources, while economic deprivation compromises health, forming a self-reinforcing cycle (Engelgau et al., 2019; Smith, 1999). In biomedicine, tumor cells and the immune system engage in mutual causation—immune surveillance exerts selective pressures that sculpt cancer clonal evolution, whereas cancer cells deploy immunosuppressive molecules to subvert immune responses, establishing a malignant “immunoediting-escape” loop

(Riaz et al., 2017). Similarly, the gut microbiota and brain maintain bidirectional communication via neuro-immune-endocrine pathways: stress-induced neural activity alters microbial composition, and dysbiosis independently disrupts brain function (Cryan et al., 2019; Foster et al., 2017). Psychologically, sleep and depression exhibit reciprocal causality: chronic insomnia elevates risks for psychiatric disorders, while over 90% of depressed patients manifest sleep disruptions consistent with insomnia (Palagini et al., 2013). Therefore, considering reverse causality is crucial for causal inference, and methods for bidirectional causal effects require further exploration.

However, in the study of bidirectional causal relationships, the presence of unobserved confoundings complicates the real-world problems. It may come with confounding bias that the true causal effect cannot be recovered, which leads to invalid causal conclusions. To address this issue, instrumental variable (IV) approach offers a potential solution for identifying causal effects by eliminating the confounding bias. The related researches on bidirectional causal inference are primarily conducted within Mendelian Randomization (MR) framework. Specifically, MR utilizes independent genetic IVs for two traits to effectively disentangle the causal relations between them, thereby separating the additional associations caused by reverse causation (Davey Smith and Hemani, 2014), which differs from the traditional studies. For example, Gao et al. (2019) regarded reverse causality as a source of confounding and used two-sample MR to explore the causal relationships between insomnia and five major psychiatric disorders. Xue and Pan (2020) refined the traditional bidirectional MR approach, enabling robust inference of causal direction between two traits even in the presence of horizontal pleiotropy. Li and Ye (2024) assessed commonly used identifiability assumptions in bidirectional MR models and proposed a new focusing framework to test bidirectional causal effects with potentially invalid instruments. Xie et al. (2024) addressed the identification of bidirectional MR models by correctly selecting valid instrument sets from observational data and developed a cluster fusion-like method to discover valid instruments.

Previous research on bidirectional causal effects based on MR primarily focuses on inferring causal direction and applications with continuous outcomes. However, binary outcomes are also frequently encountered in applied settings, particularly in epidemiological studies investigating the disease risk factors. For instance, Ten Have et al. (2003) conducted a placebo-controlled randomized trial on cholesterol levels, where participants in the treatment group listened to audio tapes delivering dietary and nursing interventions, and the binary outcome was defined as whether or not participants had high cholesterol levels. Similarly, Borracci et al. (2013) evaluated the impact of preoperative oral morphine sulfate on postoperative pain relief, where two binary outcome variables were constructed based on resting and movement pain scores using established thresholds (Lupparelli and Mattei, 2020). Compared to continuous variables, simple linear models are not applicable for binary outcomes. Clarke and Windmeijer (2012) provided a comprehensive review of IV estimation methods for binary outcomes, focusing on identification strategies that rely on linear selection models and the control function approach. However, these methods have thus far been applied exclusively within traditional unidirectional causal frameworks.

In this paper, we explore bidirectional causal frameworks with unmeasured confounding for binary variables, employing instrumental variable approaches. This paper makes the following three main contributions: First, we adopt a linear structural equation modeling (SEM) framework to capture bidirectional causal relationships between continuous latent variables. Second, we use a pair of IVs to establish the identifiability of bidirectional causal effects and derive their estimators, along with the corresponding asymptotic properties. Third, we perform sensitivity analysis to evaluate key assumptions, including the exclusion restriction and unmeasured confounding being

uncorrelated with equal variances.

The remainder of this paper is organized as follows. Section 2 presents the identification formulas and proposes the estimation methodology. Section 3 conducts sensitivity analysis for key assumptions. Section 4 reports simulation studies under various data-generating scenarios. Section 5 applies the proposed method to the Key Indicators of Heart Disease dataset. Section 6 concludes.

## 2 Notation and Framework

### 2.1 Binary bidirectional model

Let  $X \in \{0, 1\}$  denote a binary treatment (or exposure) variable, and  $Y \in \{0, 1\}$  the observed binary outcome. In observational studies, both  $X$  and  $Y$  may be influenced by background covariates, including observed variables  $C$  and  $p$ -dimensional unobserved confounders  $U$  and  $V$ . In our motivating application,  $X$  indicates the presence of coronary heart disease or myocardial infarction, and  $Y$  indicates the presence of diabetes. Previous studies (Emerging Risk Factors Collaboration et al., 2010; Henning, 2018; Katakami, 2018) have shown that individuals with diabetes ( $Y = 1$ ) are at a significantly higher risk of developing heart disease ( $X = 1$ ); conversely, complications or treatments associated with heart disease ( $X = 1$ ) may impair glucose regulation, thereby increasing the risk of developing diabetes ( $Y = 1$ ).

In such scenarios, assuming a unidirectional causal relationship (e.g.,  $X \rightarrow Y$ ) may ignore potential reverse effects, leading to biased estimates of causal effects. To more accurately capture the mutual dependence between the variables, we introduce a bidirectional causal mechanism to account for the possibility of reciprocal influences. Specifically, we assume that the latent variables follow a linear structural equation model (Hausman, 1983):

$$\begin{aligned} X^\circ &= \mu_{x0} + \beta_{y \rightarrow x} Y^\circ + \mu_{xc} C + U, & X &= \mathbb{I}(X^\circ > 0), \\ Y^\circ &= \mu_{y0} + \beta_{x \rightarrow y} X^\circ + \mu_{yc} C + V, & Y &= \mathbb{I}(Y^\circ > 0), \end{aligned} \tag{1}$$

where  $X^\circ$  and  $Y^\circ$  denote the latent continuous variables corresponding to the observed binary outcomes  $X$  and  $Y$ , respectively, and  $\mathbb{I}(\cdot)$  is the indicator function that maps the latent variables to binary responses. The covariate  $C$  is assumed to be independent of the unobserved confounders  $(U, V)$  throughout this paper (Yin et al., 2016), i.e.,  $C \perp\!\!\!\perp (U, V)$ .

In Model (1), the parameter  $\beta_{y \rightarrow x}$  represents the causal effect of  $Y^\circ$  on  $X^\circ$ , while  $\beta_{x \rightarrow y}$  denotes the causal effect of  $X^\circ$  on  $Y^\circ$ . Accordingly, this paper focuses on the identification of both parameters,  $\beta_{y \rightarrow x}$  and  $\beta_{x \rightarrow y}$ . Within the structural model (1), these two parameters can also be interpreted as the *ceteris paribus* effects of  $X^\circ$  and  $Y^\circ$ , respectively (Goldberger, 1972). When  $\beta_{y \rightarrow x} = 0$ , Model (1) reduces to a unidirectional causal model.

Model (1) presents substantial challenges due to the coexistence of the bidirectional causation, latent variable structures, and unobserved confounding. First, the reciprocal dependence between the latent variables  $X^\circ$  and  $Y^\circ$  forms a simultaneous equation system, complicating both identification and estimation, as standard regression techniques fail to recover true causal effects. Second, the observed binary variables  $X$  and  $Y$  are thresholded versions of continuous latent variables, which necessitates additional distributional assumptions to characterize the dependence structure between the observed variables and latent variables. Third, the presence of an unobserved con-

founder  $U$  and  $V$  that simultaneously affects both equations introduces endogeneity, leading to biased estimates unless properly addressed.

Therefore, to achieve either identification or partial identification, the next subsection discusses the structural and instrumental variable assumptions under which the model becomes identifiable. These assumptions form the basis for the estimation procedures developed in this paper, Section 3 further conducts sensitivity analyses to examine the robustness of our conclusions to violations of key assumptions.

## 2.2 Assumptions

We assume that the covariate vector  $C$  includes two instrumental variables (IVs),  $Z$  and  $W$ , each influencing a single causal direction. Specifically,  $Z$  directly affects  $X^\circ$  but not  $Y^\circ$ , while  $W$  directly affects  $Y^\circ$  but not  $X^\circ$ . The remaining components of  $C$ , denoted by  $Q$ , represent other observed covariates that may impact both  $X$  and  $Y$ . For notational simplicity, we omit  $Q$  in the following discussion. Figure 1(a) illustrates the structure of the bidirectional causal framework for binary variables with IVs  $Z$  and  $W$ . After incorporating two IVs  $Z$  and  $W$ , the bidirectional causal Model (1) can be simplified to the following form:

$$\begin{aligned} X^\circ &= \mu_{x0} + \beta_{y \rightarrow x} Y^\circ + \mu_{xz} Z + U, \quad X = \mathbb{I}(X^\circ > 0), \\ Y^\circ &= \mu_{y0} + \beta_{x \rightarrow y} X^\circ + \mu_{yw} W + V, \quad Y = \mathbb{I}(Y^\circ > 0). \end{aligned} \quad (2)$$

The parameters  $\mu_{xz}$  and  $\mu_{yw}$  in Model (2) characterize the effects of  $Z$  and  $W$  on the latent variables  $X^\circ$  and  $Y^\circ$ , respectively. From Model (2), it is clear that  $Z$  and  $W$  serve as valid IVs for each causal direction. Throughout this paper, we maintain this terminology for IV in the bidirectional framework because they satisfy the exclusion restriction (ER) by having no direct effects on the outcome variables, analogous to their role in traditional unidirectional models (Angrist et al., 1996). This terminology is consistent with similar treatments found in other bidirectional causal inference literature (Li and Ye, 2024; Xie et al., 2024; Xue and Pan, 2020).

In our real application of interest, the binary variables  $X$  and  $Y$  in Figure 1(a) represent two observed binary indicators:  $X$  indicates whether an individual has coronary heart disease or myocardial infarction, and  $Y$  indicates whether an individual has diabetes. The variables  $X^\circ$  and  $Y^\circ$  correspond to their underlying continuous latent variables. In this context, “whether an individual has had a stroke” can be used as the IV  $Z$  for  $X$ , and “body mass index (BMI)” can be used as the IV  $W$  for  $Y$ . This choice is based on commonly accepted medical understanding: stroke has a relatively direct effect on heart disease but only a weak direct influence on diabetes, while BMI directly affects diabetes and has a relatively minor direct impact on heart disease. Additionally, the covariates  $Q$  represent collected background characteristics such as age, gender, and race, while  $U$  and  $V$  denotes unobserved confounding factors not captured in the dataset, such as genetic predisposition and lifestyle factors.

We first impose the normality assumptions for two unobserved confounders.

**Assumption 1** (Restrictive normality). (i)  $V \sim N(0, \sigma^2)$  and  $U \sim N(0, \sigma^2)$ , (ii)  $\text{Cov}(V, U) = 0$ .

Assumption 1 imposes two conditions on the unobserved confounders  $U$  and  $V$  to facilitate identification and simplify the modeling framework. Assumption 1(i) assumes that  $U$  and  $V$  both follow normal distributions with zero means and equal variances. Assumption 1(ii) further assumes that  $U$  and  $V$  are uncorrelated, i.e., mutually independent in the normal setting. Figure 1(b)

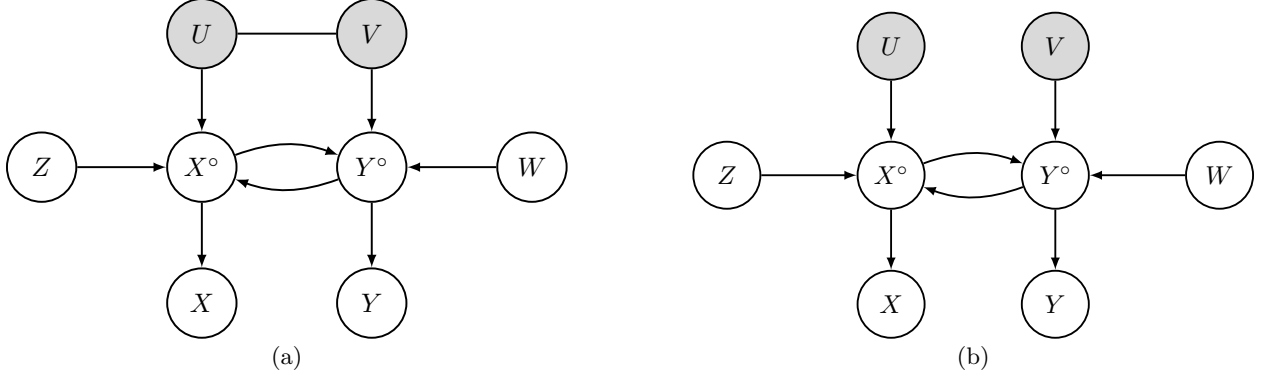


Figure 1: Graphic illustration of the bidirectional causal model (2) with instrumental variables  $Z$  and  $W$ .

shows the causal diagram that satisfies Assumption 1. This assumption is primarily introduced to simplify computation. Under this framework, Section 2.3 discusses the identification of causal effects within the bidirectional causal framework. Additionally, Section 3.1 presents the sensitivity analysis method under more general settings, applying a weaker condition than Assumption 1.

Given the constraint  $\beta_{x \rightarrow y} \beta_{y \rightarrow x} \neq 1$ , we can rewrite the structural equation Model (2) in the following reduced form:

$$\begin{aligned} X^\circ &= \theta_{x0} + \theta_{xz}Z + \theta_{xw}W + \theta_{xu}U + \theta_{xv}V, \quad X = \mathbb{I}(X^\circ > 0), \\ Y^\circ &= \theta_{y0} + \theta_{yz}Z + \theta_{yw}W + \theta_{yu}U + \theta_{yv}V, \quad Y = \mathbb{I}(Y^\circ > 0), \end{aligned} \quad (3)$$

where  $c = 1/(1 - \beta_{x \rightarrow y} \beta_{y \rightarrow x})$ ,  $\theta_{x0} = c(\mu_{x0} + \beta_{y \rightarrow x} \mu_{y0})$ ,  $\theta_{xz} = c\mu_{xz}$ ,  $\theta_{xw} = c\beta_{y \rightarrow x} \mu_{yw}$ ,  $\theta_{xu} = c$ ,  $\theta_{xv} = c\beta_{y \rightarrow x}$ ;  $\theta_{y0} = c(\beta_{x \rightarrow y} \mu_{x0} + \mu_{y0})$ ,  $\theta_{yz} = c\beta_{x \rightarrow y} \mu_{xz}$ ,  $\theta_{yw} = c\mu_{yw}$ ,  $\theta_{yu} = c\beta_{x \rightarrow y}$ , and  $\theta_{yv} = c$ . Model (3) gives the reduced form of the latent structural model (2), where  $X^\circ$  and  $Y^\circ$  are expressed as functions of exogenous variables  $(Z, W)$  and unobserved confounders  $(U, V)$ .

### 2.3 Identification

Under the structural assumptions and Assumption 1, the conditional probabilities of the two binary variables  $X$  and  $Y$  given the two observed IVs  $Z$  and  $W$  can be derived through their latent continuous representations  $X^\circ$  and  $Y^\circ$ . Under Model (3), we can derive the two observed conditional probabilities as follows, with  $\Phi(\cdot)$  being the cumulative distribution function (CDF) of standard normal distribution:

$$\begin{aligned} \text{pr}(X = 1 | Z, W) &= \text{pr}(X^\circ > 0 | Z, W) = \Phi(\xi_{x0} + \xi_{xz}Z + \xi_{xw}W), \\ \text{pr}(Y = 1 | Z, W) &= \text{pr}(Y^\circ > 0 | Z, W) = \Phi(\xi_{y0} + \xi_{yz}Z + \xi_{yw}W), \end{aligned} \quad (4)$$

where  $\lambda_1 = \text{Var}(\theta_{xu}U + \theta_{xv}V)$ ,  $\xi_{x0} = \theta_{x0}/\sqrt{\lambda_1}$ ,  $\xi_{xz} = \theta_{xz}/\sqrt{\lambda_1}$ ,  $\xi_{xw} = \theta_{xw}/\sqrt{\lambda_1}$ , and  $\lambda_2$ ,  $\xi_{y0}$ ,  $\xi_{yz}$ , and  $\xi_{yw}$  are similarly denoted. Expressions in Model (4) depend only on the observed variables  $Z$  and  $W$ , allowing us to estimate the parameters directly using observational data. We summarize the identification results in Proposition 1.

**Proposition 1.** *Under Model (2) and Assumption 1, the bidirectional causal effects are identifiable:*

$$\beta_{x \rightarrow y} = \frac{\xi_{yz}}{\xi_{xz}} \sqrt{\frac{\xi_{xw}^2 \xi_{xz}^2 - \xi_{yw}^2 \xi_{xz}^2}{\xi_{yz}^2 \xi_{yw}^2 - \xi_{yw}^2 \xi_{xz}^2}}, \quad \beta_{y \rightarrow x} = \frac{\xi_{xw}}{\xi_{yw}} \sqrt{\frac{\xi_{yz}^2 \xi_{yw}^2 - \xi_{xz}^2 \xi_{yw}^2}{\xi_{xw}^2 \xi_{xz}^2 - \xi_{xz}^2 \xi_{yw}^2}}. \quad (5)$$

where the terms  $\xi_{xz}$ ,  $\xi_{yz}$ ,  $\xi_{xw}$ , and  $\xi_{yw}$  correspond to the coefficients of  $Z$  and  $W$  in Model (4).

The detailed proof of Proposition 1 is provided in Section A of the Supplementary Materials. Proposition 1 gives the identification formulas for the causal parameters  $\beta_{x \rightarrow y}$  and  $\beta_{y \rightarrow x}$  based on the identifiable coefficients from Model (4). As shown in Equation (5), the introduction of two IVs is essential, as they differentially affect the binary variables  $X$  and  $Y$ . This difference is captured through the coefficients  $\xi_{xz}$ ,  $\xi_{yz}$ ,  $\xi_{xw}$ , and  $\xi_{yw}$  in Probit models. In addition, assuming zero covariance between  $U$  and  $V$  in Assumption 1 simplifies the parameters in Model (4), yielding a symmetric and simple identification formula (5). Proposition 1 can be interpreted as the identification result when the two unobserved confounders are uncorrelated. In Section 3.1, we will extend this framework to the scenario depicted in Figure 1(a), which incorporates the correlation between confounders, thereby deriving more general identification results.

## 2.4 Estimation and inference

Proposition 1 establishes the identification formula (5), which further allows us to estimate the bidirectional causal effects. Accordingly, we propose a two-step estimation procedure, as described in Algorithm 1.

---

### Algorithm 1 Estimation procedure for bidirectional causal effects

---

- 1: Apply maximum likelihood estimation (MLE) to the binary response models specified in Model (4), and obtain the estimated model parameters  $\hat{\xi}_{xz}$ ,  $\hat{\xi}_{yz}$ ,  $\hat{\xi}_{xw}$ , and  $\hat{\xi}_{yw}$ .
- 2: Substitute these parameter estimates into the identification formula (5) in Proposition 1, and compute the estimators of the bidirectional causal effects:

$$\hat{\beta}_{x \rightarrow y} = \frac{\hat{\xi}_{yz}}{\hat{\xi}_{xz}} \sqrt{\frac{\hat{\xi}_{xw}^2 \hat{\xi}_{xz}^2 - \hat{\xi}_{yw}^2 \hat{\xi}_{xz}^2}{\hat{\xi}_{yz}^2 \hat{\xi}_{yw}^2 - \hat{\xi}_{yw}^2 \hat{\xi}_{xz}^2}}, \quad \hat{\beta}_{y \rightarrow x} = \frac{\hat{\xi}_{xw}}{\hat{\xi}_{yw}} \sqrt{\frac{\hat{\xi}_{yz}^2 \hat{\xi}_{yw}^2 - \hat{\xi}_{xz}^2 \hat{\xi}_{yw}^2}{\hat{\xi}_{xw}^2 \hat{\xi}_{xz}^2 - \hat{\xi}_{xz}^2 \hat{\xi}_{yw}^2}}.$$


---

In the following, we provide the asymptotic properties of the estimators  $\hat{\beta}_{x \rightarrow y}$  and  $\hat{\beta}_{y \rightarrow x}$ . Let  $\boldsymbol{\Lambda} = (\xi_{x0}, \xi_{xz}, \xi_{xw}, \xi_{y0}, \xi_{yz}, \xi_{yw})^T$  denote the vector of true parameters in Model (4), and let  $\hat{\boldsymbol{\Lambda}} = (\hat{\xi}_{x0}, \hat{\xi}_{xz}, \hat{\xi}_{xw}, \hat{\xi}_{y0}, \hat{\xi}_{yz}, \hat{\xi}_{yw})^T$  denote the corresponding estimators. Based on Algorithm 1, we apply the Delta method to obtain the asymptotic distributions of  $\hat{\beta}_{x \rightarrow y}$  and  $\hat{\beta}_{y \rightarrow x}$ . The main results are summarized in Proposition 2. The detailed derivations of the asymptotic properties of the estimators  $\hat{\beta}_{x \rightarrow y}$  and  $\hat{\beta}_{y \rightarrow x}$  are provided in the Section B of the Supplementary Materials.

**Proposition 2.** *Under Model (2), suppose Assumption 1 and the regularity conditions established in Theorem 5.41 of Van der Vaart (2000) hold. Then, as  $n \rightarrow \infty$ , we have:*

$$\sqrt{n}(\hat{\boldsymbol{\Lambda}} - \boldsymbol{\Lambda}) \xrightarrow{d} N(0, \Sigma_{\boldsymbol{\Lambda}}), \quad \sqrt{n}(\hat{\beta}_{y \rightarrow x} - \beta_{y \rightarrow x}) \xrightarrow{d} N(0, \Sigma_X), \quad \sqrt{n}(\hat{\beta}_{x \rightarrow y} - \beta_{x \rightarrow y}) \xrightarrow{d} N(0, \Sigma_Y),$$

where the explicit expressions variance terms  $\Sigma_{\boldsymbol{\Lambda}}$ ,  $\Sigma_X$ , and  $\Sigma_Y$  are provided in Section B of the Supplementary Materials.

Although Proposition 2 establishes the asymptotic theory, the explicit variance expressions may be overly complicated in practice. As an alternative, we recommend using bootstrap methods to obtain the variance estimator in empirical applications.

### 3 Sensitivity Analysis

#### 3.1 Sensitivity analysis for Assumption 1

In Section 2.3, we introduced a strong normality Assumption 1 for identification. Specifically, this assumption requires that (i) the unobserved confounders  $U$  and  $V$  follow normal distributions with mean zero and equal variance  $\sigma^2$ ; and (ii) they are independent, i.e.,  $\text{Cov}(U, V) = 0$ . These two requirements are rather restrictive, since in practice it is often unrealistic to assume that the unobserved confounders in the two models have identical variances and are completely independent. In this subsection, while still utilizing the IVs, we conduct a sensitivity analysis for Assumption 1. We propose the following new assumption that is weaker than Assumption 1, allowing  $U$  and  $V$  to have different variances and be potentially correlated.

**Assumption 2** (Normality). (1)  $V \sim N(0, \sigma^2)$  and  $U \sim N(0, \gamma_1 \sigma^2)$ , (2)  $\text{Cov}(V, U) = \gamma_2 \sigma^2$ .

To quantify the influence of the relationship between unobserved confounders  $U$  and  $V$ , we introduce two sensitivity parameters in Assumption 2:  $\gamma_1 = \text{Var}(U)/\text{Var}(V)$  and  $\gamma_2 = \text{Cov}(U, V)/\text{Var}(V)$ . The parameter  $\gamma_1$  quantifies the relative strength of the variance of  $U$  compared to  $V$ , while  $\gamma_2$  describes the impact of the covariance between  $U$  and  $V$  relative to the variance of  $V$ . It is clear that two sensitivity parameters satisfying  $\gamma_1 \geq \gamma_2^2$ . Specifically, when  $\gamma_1 = 1$  and  $\gamma_2 = 0$ , Assumption 2 is equivalent to Assumption 1. The two parameters enable us to investigate how the relative variances of  $U$  and  $V$ , together with their covariance  $\text{Cov}(U, V)$ , influence the identification and estimation of the bidirectional causal effects.

In this context, we introduce two notations:  $k_1 \equiv \xi_{yz}/\xi_{xz}$  and  $k_2 \equiv \xi_{xw}/\xi_{yw}$ , to simplify the subsequent discussion. They represent the ratios of the Probit regression coefficients of  $X$  on the observed variables  $(Z, W)$  and  $Y$  on  $(Z, W)$ , respectively. The following proposition provides the identification results:

**Proposition 3.** *Under Model (2) and Assumption 2, given the sensitivity parameters  $\gamma_1$  and  $\gamma_2$ , we obtain the identification formula for the causal effects between  $X$  and  $Y$ :*

$$\beta_{x \rightarrow y} = \frac{\gamma_2 k_1 (k_2 - k_1) \pm k_1 \sqrt{\Delta_1}}{\gamma_1^2 (k_1^2 - 1)}, \quad \beta_{y \rightarrow x} = \frac{k_1 k_2}{\beta_{x \rightarrow y}} = \frac{\gamma_1^2 k_2 (k_1^2 - 1)}{\gamma_2 (k_2 - k_1) \pm \sqrt{\Delta_1}}, \quad (6)$$

where  $\Delta_1 = \gamma_1^2 k_1^2 k_2^2 - \gamma_1^2 k_1^2 - \gamma_1^2 k_2^2 + \gamma_1^2 + \gamma_2^2 k_1^2 - 2\gamma_2^2 k_1 k_2 + \gamma_2^2 k_2^2$ , and the solution satisfies  $\text{sgn}(\beta_{x \rightarrow y}) = \text{sgn}(k_1)$ .

When the unobserved confounders are correlated and their covariances are unequal, the causal structure becomes more complex, making it more difficult to distinguish the bidirectional causal effects. Proposition 3 shows that, in this case, the identification of bidirectional causal effects largely depends on the discriminant of  $\Delta_1$ . Notably, this discriminant can not only be empirically tested with data but also be used to compute the bidirectional causal effects given specified sensitivity parameters. When  $\Delta_1 > 0$ , two solutions may arise in practice. Since the sign of  $\beta_{x \rightarrow y}$  can be determined as  $k_1$ , it can be used to identify the true causal effect direction, which is particularly useful when the two solutions yield opposite signs. In practice, by varying the sensitivity parameters  $\gamma_1$  and  $\gamma_2$ , we can investigate how changes in the structure of confounders influence the estimation of bidirectional causal effects. The specific proof of Proposition 3 is presented in Section C of the Supplementary Materials.

Similarly, we can construct plugging-in based estimators and establish the corresponding asymptotic theory by following the approach in Section 2.4. For simplicity, we omit the details here.

### 3.2 Further sensitivity analysis for ER assumption

Selecting valid instrumental variables that satisfy Model (2) poses significant challenges in practice. A key concern is that the instrumental variables  $Z$  may have direct effects on  $Y^\circ$ , and  $W$  may have direct effects on  $X^\circ$ . To address this issue, we extend the sensitivity analysis framework introduced in Section 3.1 by incorporating sensitivity parameters for the instrumental variables and evaluating the robustness of our results to violations of the exclusion restriction assumption.

In addition to the sensitivity parameters  $\gamma_1$  and  $\gamma_2$  in Assumption 2, we introduce two additional sensitivity parameters,  $\eta$  and  $\delta$ , to account for potential violations of the IVs. These parameters represent the extent to which the instrumental variables  $Z$  and  $W$  exert direct effects on  $Y^\circ$  and  $X^\circ$ , respectively. The modified structural model is given by:

$$\begin{aligned} X^\circ &= \mu_{x0} + \beta_{y \rightarrow x} Y^\circ + \mu_{xz} Z + \delta W + U, \quad X = \mathbb{I}(X^\circ > 0), \\ Y^\circ &= \mu_{y0} + \beta_{x \rightarrow y} X^\circ + \eta Z + \mu_{yw} W + V, \quad Y = \mathbb{I}(Y^\circ > 0). \end{aligned} \quad (7)$$

When the sensitivity parameters  $\eta$  and  $\delta$  are set to zero, the modified Model (7) reduces to Model (2). Given Assumption 2, we can derive a Probit model similar to Model (4). While the coefficients are the same as in the previous model, as they correspond to the regression coefficients in the Probit model, they now involve more complex expressions due to the additional direct effects  $\eta$  and  $\delta$  introduced in Model (7). To illustrate these differences in parameter complexity, we present the key parameter expressions below:

$$\begin{aligned} \text{pr}(X = 1 | Z, W) &= \text{pr}(X^\circ > 0 | Z, W) = \Phi(\xi_{x0} + \xi_{xz} Z + \xi_{xw} W), \\ \text{pr}(Y = 1 | Z, W) &= \text{pr}(Y^\circ > 0 | Z, W) = \Phi(\xi_{y0} + \xi_{yz} Z + \xi_{yw} W), \end{aligned}$$

where  $\xi_{x0} = \theta_{x0}/\sqrt{\lambda_1}$ ,  $\xi_{xz} = \theta_{xz}^*/\sqrt{\lambda_1}$ ,  $\xi_{xw} = \theta_{xw}^*/\sqrt{\lambda_1}$ ,  $\theta_{xz}^* = c(\mu_{xz} + \beta_{y \rightarrow x} \eta)$ ,  $\theta_{xw}^* = c(\delta + \beta_{y \rightarrow x} \mu_{yw})$ ,  $\theta_{yz}^* = c(\beta_{x \rightarrow y} \mu_{xz} + \eta)$ , and  $\theta_{yw}^* = c(\beta_{x \rightarrow y} \delta + \mu_{yw})$  and similarly for  $\xi_{y0}$ ,  $\xi_{yz}$ , and  $\xi_{yw}$ . The coefficients  $c$ ,  $\lambda_1$ ,  $\lambda_2$ ,  $\theta_{x0}$ ,  $\theta_{y0}$ ,  $\theta_{xu}$ ,  $\theta_{xv}$ ,  $\theta_{yu}$ , and  $\theta_{yv}$  are already defined in (3) and (4).

Given the sensitivity parameters  $\eta$  and  $\delta$ , to establish identifiable results, we introduce reparameterizations of the sensitivity parameters, which will be used in the following theoretical results. We define  $\eta_0 = \eta/\mu_{xz}$ , which represents the relative strength of the effect of  $Z$  on  $(X^\circ, Y^\circ)$ , and  $\delta_0 = \delta/\mu_{yw}$ , which represents the relative strength of the effect of  $W$  on  $(X^\circ, Y^\circ)$ .

**Proposition 4.** *Under Model (7) and Assumption 2, for any given sensitivity parameters  $(\gamma_1, \gamma_2, \eta_0, \delta_0)$ , the bidirectional causal effect  $\beta_{y \rightarrow x}$  can be partially identified by solving the following univariate quartic equation:  $F(\beta_{y \rightarrow x}; \xi_{xz}, \xi_{xw}, \xi_{yz}, \xi_{yw}, \eta_0, \delta_0, \gamma_1, \gamma_2) = 0$ , where the detail discussion of  $F(\cdot)$  are provided in Section D.1 of the Supplementary Materials. Once  $\beta_{y \rightarrow x}$  is obtained, the corresponding causal effect  $\beta_{x \rightarrow y}$  can be identified through the following explicit formula:*

$$\beta_{x \rightarrow y} = \frac{\xi_{xz} \xi_{yw} \delta_0 \eta_0 - \xi_{yz} \xi_{xw} - \xi_{xz} \xi_{yw} \eta_0 \beta_{y \rightarrow x} + \xi_{yz} \xi_{xw} \eta_0 \beta_{y \rightarrow x}}{\xi_{xz} \xi_{yw} \beta_{y \rightarrow x} - \xi_{yz} \xi_{xw} \eta_0 \delta_0 \beta_{y \rightarrow x} + \xi_{xz} \xi_{yw} \delta_0 - \xi_{yz} \xi_{xw} \delta_0}.$$

Building upon Proposition 3, Proposition 4 incorporates the direct effect parameters  $\eta$  and  $\delta$  to conduct a more comprehensive sensitivity analysis under the Model (7). By utilizing the univariate quartic equation provided in Proposition 4, we can obtain corresponding estimates of the causal effects under any combination of sensitivity parameters  $(\gamma_1, \gamma_2, \eta_0, \delta_0)$ . This enables us to evaluate the impact of different confounding scenarios induced by unobserved confounders  $U$  and  $V$ , as

well as violations of instrumental variable assumptions related to  $Z$  and  $W$ , on the causal effect estimates.

However, solving the quartic equation in Proposition 4 poses significant computational challenges in practical applications. Intuitively, this difficulty arises because the direct effects of  $Z$  and  $W$  on  $X^\circ$  and  $Y^\circ$  are inherently intertwined, making it challenging to disentangle their individual contributions to the causal effects. To make the sensitivity analysis more tractable and practically interpretable, we examine three special cases that yield simplified analytical expressions, thereby facilitating implementation in empirical applications. Figure 2 illustrates the causal frameworks under the sensitivity analysis settings specified in the following three corollaries.

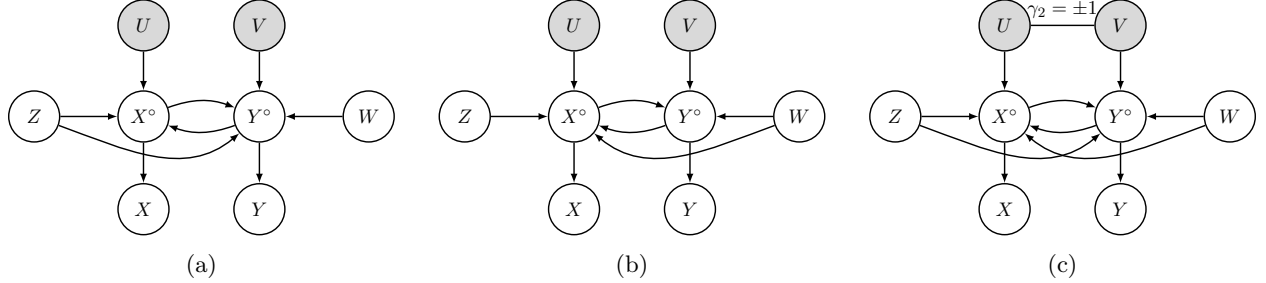


Figure 2: Three graphical illustrations of Model (7).

**Corollary 1.** Consider the setting with  $\delta_0 = 0$ ,  $\gamma_1 = 1$ ,  $\gamma_2 = 0$ , and arbitrary  $\eta_0$  (illustrated in Figure 2(a)). The bidirectional causal effects are identified by solving the quadratic equation:

$$\beta_{y \rightarrow x} = \frac{-s_2 \pm \sqrt{s_2^2 - 4s_1s_3}}{2s_1}, \quad \beta_{x \rightarrow y} = \eta_0(t_1t_2 - 1) + \frac{2s_1t_1t_2}{-s_2 \pm \sqrt{s_2^2 - 4s_1s_3}},$$

where  $t_1 = \xi_{xw}/\xi_{xz}$ ,  $t_2 = \xi_{yz}/\xi_{yw}$ ,  $t_3 = \xi_{xz}/\xi_{yz}$ ,  $t_4 = \xi_{xw}/\xi_{yw}$ ,  $s_1 = \eta_0^2(t_1t_2 - 1)^2 - t_1t_2t_3t_4 + 1$ ,  $s_2 = 2t_1t_2\eta_0(t_1t_2 - 1)$ , and  $s_3 = t_1t_2(t_1t_2 - t_3t_4)$ . The solution satisfies  $\text{sgn}(\beta_{y \rightarrow x}) = \text{sgn}(t_4)$ .

**Corollary 2.** Consider the setting with  $\eta_0 = 0$ ,  $\gamma_1 = 1$ ,  $\gamma_2 = 0$ , and arbitrary  $\delta_0$  (illustrated in Figure 2(b)). The bidirectional causal effects are identified by solving the quadratic equation:

$$\beta_{y \rightarrow x} = \frac{-s_5 \pm \sqrt{s_5^2 - 4s_4s_6}}{2s_4}, \quad \beta_{x \rightarrow y} = \delta_0(t_1t_2 - 1) + \frac{2s_4t_1t_2}{-s_5 \pm \sqrt{s_5^2 - 4s_4s_6}},$$

where  $t_1$ ,  $t_2$ ,  $t_3$  and  $t_4$  are already defined in Corollary 1,  $s_4 = t_3t_4 + t_3t_4\delta_0^2(t_1t_2 - 1)^2 - t_1t_2$ ,  $s_5 = 2t_1t_2t_3t_4\delta_0(t_1t_2 - 1)$ , and  $s_6 = t_1t_2(t_1t_2t_3t_4 - 1)$ . The solution satisfies  $\text{sgn}(\beta_{x \rightarrow y}) = \text{sgn}(t_3)$ .

Corollary 1 examines the identification of bidirectional causal effects when  $Z$  has direct effects of different magnitudes on  $Y^\circ$ , under the assumptions that  $W$  is a valid instrumental variable and the unobserved confounders  $U$  and  $V$  are independent. Corollary 2 is similar, and we omit the discussion for simplicity. This approach is motivated by sensitivity analyses for violations of the ER assumption in traditional instrumental variable frameworks (Angrist et al., 1996). It is worth noting that although two solutions exist in these contexts, similar to Proposition 3, we can sometimes uniquely determine the bidirectional causal effects by utilizing the sign of  $\beta_{x \rightarrow y}$ .

Beyond the scenarios in Corollaries 1 and 2, it is necessary to explore cases where the unobserved confounders  $U$  and  $V$  are correlated, while simultaneously allowing both  $Z$  and  $W$  to have direct effects on  $X^\circ$  and  $Y^\circ$ .

**Corollary 3.** We introduce the signal-to-noise ratios  $\eta_0 = \eta/\sigma$  and  $\delta_0 = \delta/\sigma$  to reparameterize  $\eta$  and  $\delta$  in Model (7), and then consider the setting with  $\gamma_1 = 1$ ,  $\gamma_2 = 0$ , and arbitrary  $\delta_0$  and  $\eta_0$  (as illustrated in Figure 2(c)). Consequently, when  $\beta_{x \rightarrow y}\beta_{y \rightarrow x} < 1$ , the identification expressions for the bidirectional causal effects are given by:

$$\beta_{y \rightarrow x} = \frac{(\xi_{yz} - \xi_{xz})(\xi_{xw} - \delta_0)}{(\xi_{xw} - \xi_{yw})(\xi_{xz} - \eta_0)}, \quad \beta_{x \rightarrow y} = \frac{(\xi_{xw} - \xi_{yw})(\xi_{yz} - \eta_0)}{(\xi_{yz} - \xi_{xz})(\xi_{yw} - \delta_0)}. \quad (8)$$

When  $\beta_{x \rightarrow y}\beta_{y \rightarrow x} > 1$ , the identification expressions for the bidirectional causal effects are given by:

$$\beta_{y \rightarrow x} = \frac{(\xi_{yz} - \xi_{xz})(\xi_{xw} + \delta_0)}{(\xi_{xw} - \xi_{yw})(\xi_{xz} + \eta_0)}, \quad \beta_{x \rightarrow y} = \frac{(\xi_{xw} - \xi_{yw})(\xi_{yz} + \eta_0)}{(\xi_{yz} - \xi_{xz})(\xi_{yw} + \delta_0)}. \quad (9)$$

Corollary 3 considers a special symmetric design, where it is assumed that the unobserved confounders  $U$  and  $V$  are perfectly positively or negatively correlated, and direct causal paths are simultaneously introduced to both instrumental variables. However, unlike Proposition 4, Corollary 1 and Corollary 2, as shown in Section D.5 of the Supplementary Materials, when the parameterization  $\eta_0 = \eta/\mu_{xz}$  and  $\delta_0 = \delta/\mu_{yw}$  is applied, two distinct identification expressions for the bidirectional causal effects emerge, indicating that the result is also partial identification. However, under this reparameterization, we cannot, as in Proposition 3, Corollary 1 and 2, determine the sign of the solution from the two possible solutions, making it difficult to find a unique solution.

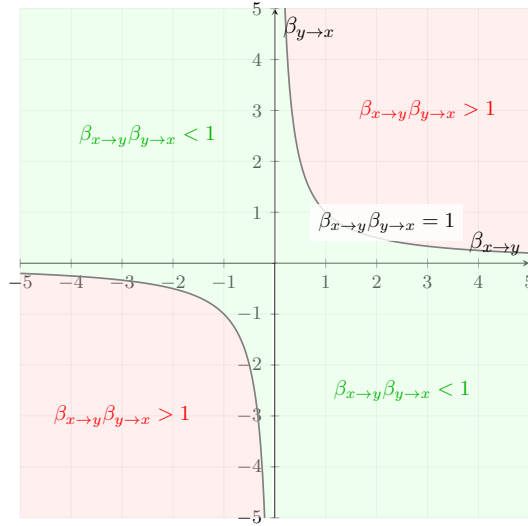


Figure 3: Corresponding regional division for the application of causal effect identification expressions.

Therefore, as described in Corollary 3, we adopt a signal-to-noise ratio parameterization,  $\eta_0 = \eta/\sigma$  and  $\delta_0 = \delta/\sigma$ , which reflects the relative magnitude of the coefficients  $\eta$  and  $\delta$  compared to the standard deviation of the unobserved confounders. Under this setting, although two possible solutions for the bidirectional causal effects still exist, since the relative magnitude of  $\beta_{x \rightarrow y}\beta_{y \rightarrow x}$  with respect to 1 cannot be determined, the conditions for solutions (8) and (9) provide more informative guidance for unique identification. As shown in Figure 3, when the parameters are more likely to fall within the green region, i.e.,  $\beta_{x \rightarrow y}\beta_{y \rightarrow x} < 1$ , we apply Equation (8) for identification based on

the sensitivity parameters. Conversely, in the red region, i.e.,  $\beta_{x \rightarrow y} \beta_{y \rightarrow x} > 1$ , we apply Equation (9) for identification. For example, in practice, when it is reasonable to assume that  $\beta_{x \rightarrow y}$  and  $\beta_{y \rightarrow x}$  have opposite signs, the solution (8) should be chosen. The complete proofs of Corollaries 1 to 3 are provided in Sections D.2 to D.4 of the Supplementary Materials B.

## 4 Numerical Experiments

### 4.1 Simulation studies

In this section, we conduct numerical simulations to evaluate the finite sample performance of the proposed method in Section 2. The data-generating process is as follows:

1. Generate the observed covariate  $Q$  from a standard normal distribution,  $Q \sim N(0, 1)$ ;
2. Generate the unobserved confounders  $U$  and  $V$  from a normal distribution according to Assumption 1, i.e.,  $U \sim N(0, \sigma^2)$ ,  $V \sim N(0, \sigma^2)$  where  $\sigma = 0.75$ ;
3. For the instrumental variables  $Z$  and  $W$ , we consider the following two distributional scenarios:
  - Scenario 1:  $Z \sim N(0, 1)$ ,  $W \sim N(0, 1)$ ;
  - Scenario 2:  $Z \sim \text{Unif}(-1, 1)$ ,  $W \sim \text{Unif}(-1, 1)$ ;
4. Generate the continuous latent variables  $X^\circ$  and  $Y^\circ$  based on the linear structural Model (2), and then map them to the observed binary variables  $X$  and  $Y$  using the threshold rule. We set  $\mu_{x0} = \mu_{y0} = 0$  and the true parameter values in Model (2) are given by:  $\beta_{y \rightarrow x} = 0.45$ ,  $\beta_{x \rightarrow y} = -0.25$ ,  $\mu_{xz} = \mu_{yw} = 0.65$ , and the coefficient of the omitted covariate  $Q$  in Model (2) is  $\mu_{xq} = \mu_{yq} = 0.15$ .

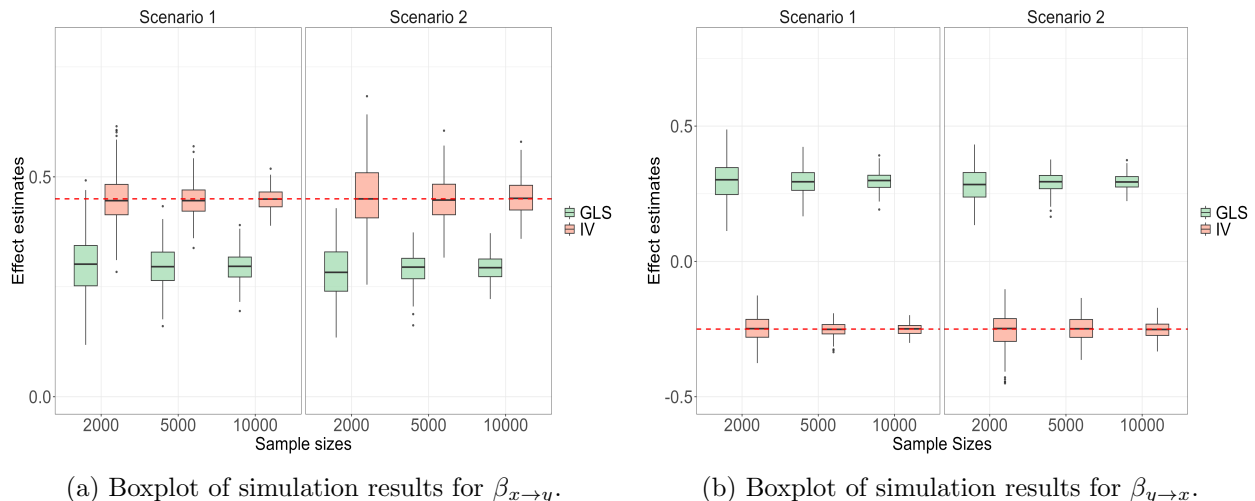


Figure 4: Boxplot of simulation results under bidirectional framework.

For the two data-generating scenarios, we consider two estimation methods with sample sizes  $N = 2000, 5000$ , and  $10000$ . The first method (GLS) is the direct regression approach, where we fit two Probit models: one by regressing  $Y$  on  $(X, Z, W, Q)$ , and another by regressing  $X$  on  $(Y, Z, W, Q)$ , the resulting coefficients on  $X$  and  $Y$  are then interpreted as estimates of  $\hat{\beta}_{x \rightarrow y}$  and  $\hat{\beta}_{y \rightarrow x}$ , respectively. The second method (IV) is Algorithm 1 proposed in this paper. Based on the simulated data for  $X, Y, Z, W$  and  $Q$ , we perform Probit regression to estimate the coefficients in Equation (4), namely,  $\xi_{xz}, \xi_{xw}, \xi_{yz}$  and  $\xi_{yw}$ . These estimated coefficients are then substituted into the identification formula (5) to obtain the estimates  $\hat{\beta}_{x \rightarrow y}$  and  $\hat{\beta}_{y \rightarrow x}$ .

The estimation results show that the proposed method performs well across both scenarios, yielding consistent estimates. In contrast, the direct regression approach produces estimates that deviate significantly from the true values in both scenarios. Furthermore, we compute the standard deviation and bias of the proposed estimators over 200 repeated simulations. Figure 4 presents the simulation results for the bidirectional causal effect, where the red represents our proposed method and the green represents the naive regression method. The corresponding numerical results are summarized in Table 1. It can be observed that the standard deviation and bias of the estimators decrease as the sample size increases across both scenarios.

Table 1: Simulation study results: standard deviation and bias of bidirectional causal effect estimators across scenarios and methods. All values are multiplied by  $10^4$ .

		Sample Size	Scenario 1			Scenario 2		
			2000	5000	10000	2000	5000	10000
GLS	$\hat{\beta}_{x \rightarrow y}$	bias	-1510	-1550	-1540	-1640	-1590	-1570
		sd	724	475	358	635	379	288
	$\hat{\beta}_{y \rightarrow x}$	bias	5490	5450	5460	5370	5420	5440
		sd	718	480	355	637	383	289
IV	$\hat{\beta}_{x \rightarrow y}$	bias	-2	-9	10	80	25	-8
		sd	535	355	242	941	504	407
	$\hat{\beta}_{y \rightarrow x}$	bias	-45	-9	-7	10	-29	-31
		sd	500	265	208	755	433	354

## 4.2 Sensitivity analysis for Assumption 1

In this section, we conduct a sensitivity analysis of Assumption 1, focusing on the influence of both the variance relationship and covariance of the unobserved confounders  $U$  and  $V$  on the estimation results. Accordingly, we modify the second step of the data generation process in Section 4.1 as follows: Under Assumption 2, we generate the unobserved confounders  $U$  and  $V$ , where  $U \sim N(0, \gamma_1 \sigma^2)$ ,  $V \sim N(0, \sigma^2)$ , and  $\text{cov}(U, V) = \gamma_2 \sigma^2$ , with  $\sigma = 0.75$ . The parameter  $\gamma_1$  varies within the range  $(0.1, 1)$  at intervals of 0.02, while  $\gamma_2$  varies within the range  $(-0.6, 0.6)$  at intervals of 0.02. All other settings remain consistent with Section 4.1.

For each parameter combination  $(\gamma_1, \gamma_2)$ , we perform 200 repeated simulations and obtain a series of point estimates using the proposed method. Figure 5 presents the bias and standard deviation of bidirectional causal effect estimates across different sensitivity parameter values for a

sample size of  $N = 10000$ . The black curve corresponds to the truncation of the parabola defined by  $\gamma_1 = \gamma_2^2$ . As stated in Proposition 3, within the parabola, specific point estimates of the causal effects can be obtained once the two sensitivity parameter values are determined.

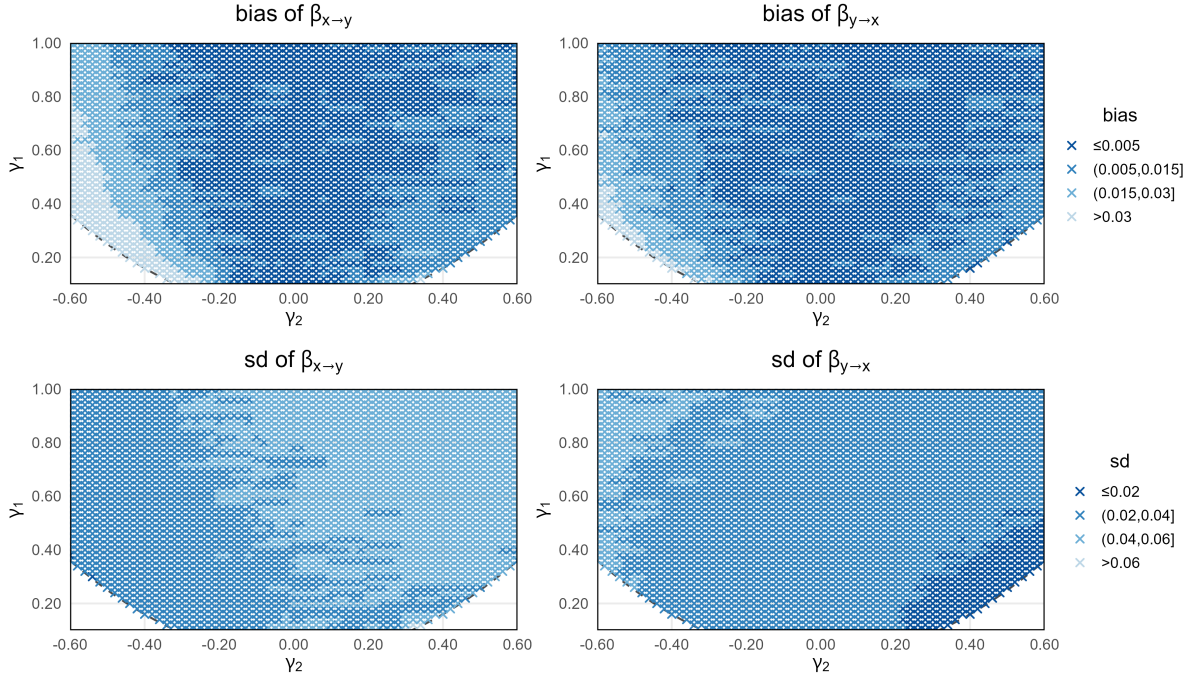


Figure 5: Bias and standard deviation estimation results.

The first row of Figure 5 presents the bias of the bidirectional causal effect estimates  $\beta_{x \rightarrow y}$  and  $\beta_{y \rightarrow x}$  across different combinations of sensitivity parameters  $(\gamma_1, \gamma_2)$ . The color gradient from light to dark represents the magnitude of the bias. The second row of Figure 5 displays the standard deviations of the estimates. Both subfigures in the first row show that the bias remains consistently small (mainly represented by lighter colors) across a wide range of sensitivity parameter combinations, especially in the central region where  $\gamma_1$  and  $\gamma_2$  are close to zero. The bias results for  $\beta_{x \rightarrow y}$  and  $\beta_{y \rightarrow x}$  exhibit similar characteristics, with both showing minimal bias in the central regions where  $\gamma_1$  and  $\gamma_2$  are close to zero. The bias tends to slightly increase toward the extreme values of the parameter space, particularly in the corners where both  $|\gamma_1|$  and  $|\gamma_2|$  are large. However, even in these extreme scenarios, the bias remains within acceptable estimation performance ( $\leq 0.03$  according to the legend). Furthermore, the corresponding standard deviations exhibit varying performances across different parameter combinations, but overall, they remain consistently below 0.06, indicating the method's robustness to strong confounding.

### 4.3 Sensitivity analysis simulation for ER assumption

This section conducts numerical simulations for the three instrumental variable sensitivity analysis settings discussed in Section 3.2, aiming to assess the impact of violating the specification of Model (2), specifically by adding direct effect paths from the instrumental variables to the target variables, on causal effect estimation under finite sample sizes. The basic simulation setup re-

mains consistent with that in Section 4.1. However, we modify certain settings to correspond with Corollaries 1 to 3 in Section 3.2, which are specifically shown as follows:

Case 1: Following the configuration in Corollary 1, we set  $\delta_0 = 0$ ,  $\gamma_1 = 1$ ,  $\gamma_2 = 0$ , and consider an arbitrary sensitivity parameter  $\eta_0$ . The parameter  $\eta_0$  varies within the range  $[-0.16, 0.16]$  with increments of 0.02.

Case 2: Following the configuration in Corollary 2, we set  $\eta_0 = 0$ ,  $\gamma_1 = 1$ ,  $\gamma_2 = 0$ , and consider an arbitrary sensitivity parameter  $\delta_0$ . The parameter  $\delta_0$  varies within the range  $[-0.16, 0.16]$  with increments of 0.02.

Case 3: Following the configuration in Corollary 3, we set  $\gamma_1 = 1$ ,  $\gamma_2 = 1$ , and consider arbitrary sensitivity parameters  $\eta_0$  and  $\delta_0$ . Both parameters are constrained such that  $\eta_0 = \delta_0$ , and they vary within the range  $[-0.16, 0.16]$  with increments of 0.02.

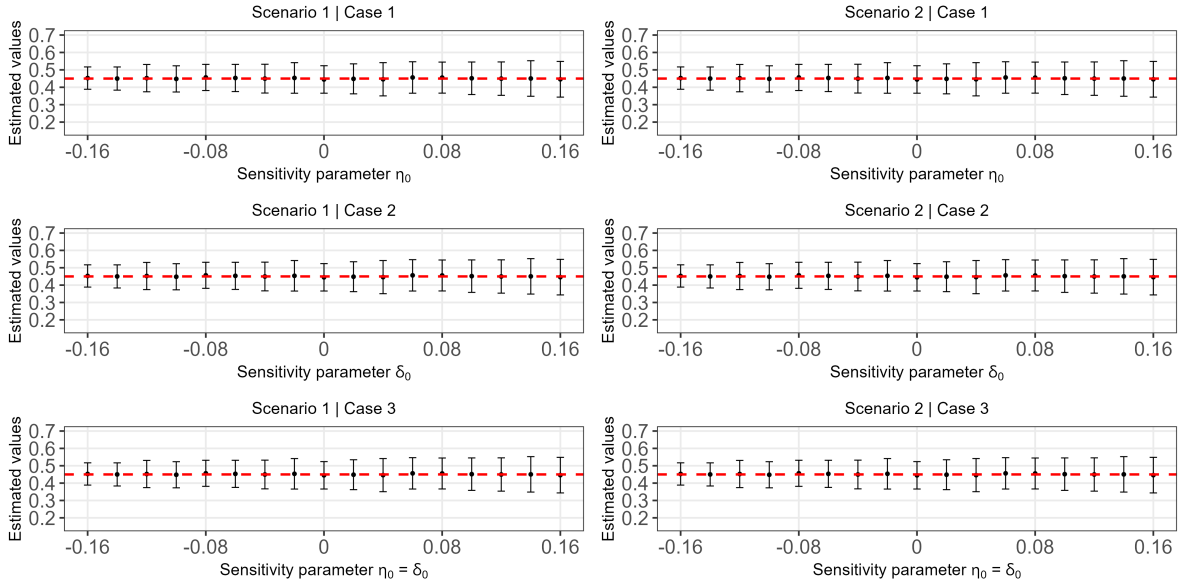


Figure 6: The point estimate and 95% confidence interval results of  $\beta_{x \rightarrow y}$ .

Based on the simulation results from 200 repeated simulations under different combinations of parameters and data-generating scenarios, we plot error bar graphs in Figures 6. The red dashed lines in the figures represent the given true value of the causal effect parameter. It can be observed that across different parameter values, the point estimates under both data-generating scenarios remain consistently stable around the true value. Furthermore, when the arbitrary sensitivity parameters in the first two settings are changed to zero, the estimation results are equivalent to those under the specification of Model (2). Simultaneously, as the sample size increases, the estimation error decreases accordingly. These findings demonstrate that the proposed method retains its robustness even when the instrumental variables  $Z$  and  $W$  violate the assumptions of Model (2) to some extent. Here, we present the results for  $\beta_{x \rightarrow y}$  under three settings with a sample size of  $N = 10000$ . Simulation results for other sample sizes and for  $\beta_{y \rightarrow x}$  are provided in detail in Section E of the Supplementary Materials.

## 5 Application

### 5.1 Description

According to the Centers for Disease Control and Prevention (CDC), heart disease is the leading cause of death among most racial groups in the United States, including African Americans, American Indians/Alaska Natives, and Whites. In addition, nearly half (47%) of US adults have at least one of the three major risk factors: high blood pressure, high cholesterol, or smoking. Other important risk factors include diabetes, obesity (high body mass index, BMI), physical inactivity, and excessive alcohol consumption.

In this study, we apply our proposed method to investigate the bidirectional causal relationship between heart disease and diabetes. The data we use come from the 2023 release of the Behavioral Risk Factor Surveillance System (BRFSS) by the CDC. This dataset contains 319795 records and 18 variables, including indicators for coronary heart disease or myocardial infarction, diabetes status, smoking, BMI, and other health-related factors. We focus on the bidirectional causal relationship between  $X$  (coronary heart disease or myocardial infarction) and  $Y$  (diabetes). The remaining 16 variables (e.g., age, gender, race) are provided in Table 2. Given that the BMI values in the dataset are much larger in scale compared to the binary variables (with values 0 and 1), we standardize the BMI variable prior to analysis.

Table 2: Descriptive statistics for variables related to heart disease and diabetes.

Variable	Type	Mean/Rate	Variable	Type	Mean/Rate
BMI	Continuous	28.325	Race	Categorical	1.564
Smoking	Binary	41.25%	AgeCategory	Categorical	7.515
AlcoholDrinking	Binary	6.81%	PhysicalActivity	Binary	77.54%
Stroke	Binary	3.77%	GenHealth	Categorical	2.595
PhysicalHealth	Categorical	3.372	SleepTime	Categorical	7.097
MentalHealth	Categorical	3.898	Asthma	Binary	13.41%
DiffWalking	Binary	13.89%	KidneyDisease	Binary	3.68%
Sex	Binary	47.53%	SkinCancer	Binary	9.32%

Since stroke is clinically closely associated with the onset of heart disease but has limited direct impact on diabetes, and individuals with higher BMI are more likely to develop diabetes while BMI has a limited direct effect on heart disease, we treat “stroke” as the instrumental variable  $Z$  for  $X^\circ$  and “BMI” as the instrumental variable  $W$  for  $Y^\circ$ .

### 5.2 Analysis under the assumptions in Section 2.3

For the heart disease dataset, we apply our proposed method under Assumption 1 to estimate the bidirectional causal effects between heart disease and diabetes, while also providing results from the direct regression approach for comparison. Based on 200 bootstrap replications, we compute the standard deviations (SD) and 95% confidence intervals for  $\beta_{x \rightarrow y}$  and  $\beta_{y \rightarrow x}$ . All results are presented in Table 3.

We find that both point estimates are positive, indicating a bidirectional positive association between  $X$  and  $Y$ , that is, coronary heart disease or myocardial infarction may have a significant positive effect on diabetes, and vice versa. The 95% confidence intervals obtained via bootstrap do not include zero, further supporting the presence of statistically significant positive effects in both

Table 3: Summary of bidirectional causal effect estimates in the heart disease application.

		Estimate	SD	95% Confidence Interval
GLS	$\hat{\beta}_{x \rightarrow y}$	0.2510	0.0097	[0.2321, 0.2698]
	$\hat{\beta}_{y \rightarrow x}$	0.2554	0.0090	[0.2379, 0.2729]
IV	$\hat{\beta}_{x \rightarrow y}$	0.3108	0.0262	[0.2594, 0.3621]
	$\hat{\beta}_{y \rightarrow x}$	0.1786	0.0154	[0.1484, 0.2088]

directions. These findings imply that the onset of heart disease may elevate the risk of developing diabetes, potentially due to physiological stress, inflammation, or lifestyle changes following a cardiovascular event. Conversely, individuals with diabetes may face an increased risk of heart disease, consistent with existing clinical evidence that links poor glycemic control to vascular damage and atherosclerosis (Brownlee, 2001). In addition, the direct regression approach yields point estimates with the same direction of effect, suggesting that the estimation results obtained using our proposed method are robust and reliable.

### 5.3 Sensitivity analysis for for Assumption 1

In practice, it is challenging to determine the actual relative strength of the unobserved confounding affecting the two target variables of interest – “heart disease” and “diabetes”. Therefore, parallel to Section 4.2, we extend the study based on Assumption 1 in Section 5.2 by introducing parameters  $\gamma_1$  and  $\gamma_2$  to conduct a sensitivity analysis on this dataset. This aims to evaluate the accuracy of the proposed method in assessing possible real-world confounding scenarios. We vary  $\gamma_1$  over the range  $[0.5, 3]$  at intervals of 0.05, and  $\gamma_2$  over  $[-1.5, 1.5]$  at intervals of 0.1. Based on the identification formula (6) provided in Proposition 3, a series of estimates within the identifiable region are obtained. Figure 7 displays these estimates under different parameter combinations and uses color shading to represent their magnitudes and variations.

As can be seen from Figure 7, under different values of the parameter combinations  $(\gamma_1, \gamma_2)$ , the point estimates obtained from the empirical data are consistently positive. Moreover, according to the numerical range displayed in the figure, the range of the estimates when the absolute values of both parameters are close to zero is relatively consistent with the confidence interval obtained in Section 5.2. Overall, given the limited information on unobserved confounders, the method proposed in this paper can provide a reliable range for causal effect estimates, offering a practical reference value for real-world applications. Moreover, if more comprehensive information on confounders becomes available, such as knowledge from domain experts regarding the relative strength of the influence of unobserved confounders on heart disease and diabetes, the range of the causal effect point estimates can be further narrowed.

### 5.4 Sensitivity analysis for ER assumption

In Sections 5.2 and 5.3, we estimate the bidirectional causal effects between heart disease and diabetes and conduct corresponding sensitivity analyses under Assumption 1 and its weaker version, respectively. These investigations are carried out within the framework of Model (2), wherein the

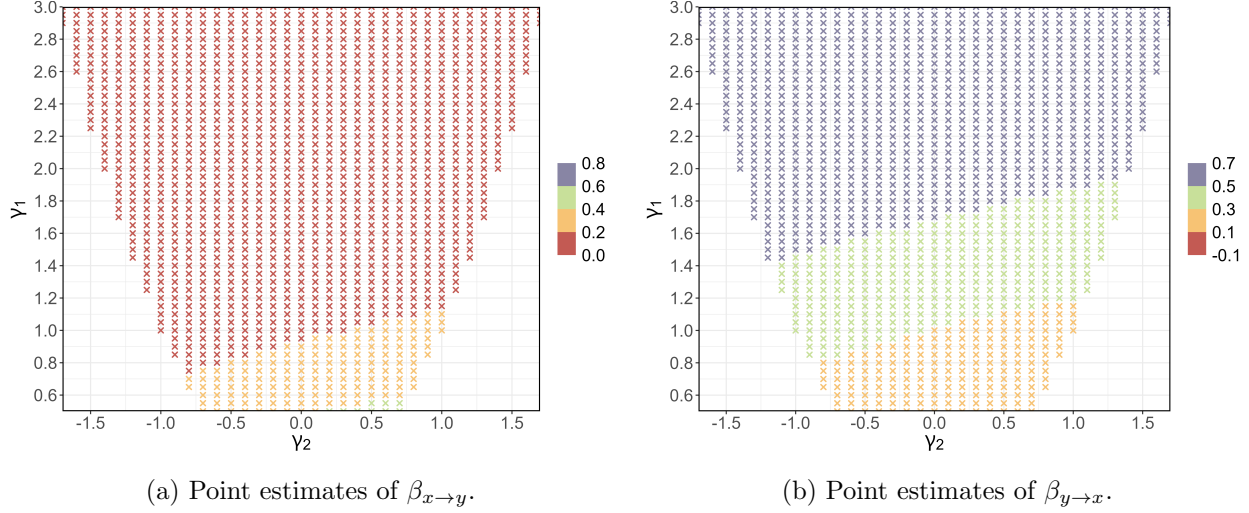


Figure 7: Sensitivity analysis results for various parameter setting with the heart disease and diabetes dataset.

selected variables—"stroke" and "BMI"—are assumed to be valid instrumental variables for heart disease and diabetes, respectively. Therefore, building upon Model (7), we further incorporate a sensitivity analysis addressing potential violations of the ER assumption for IVs in this dataset. This analysis follows the three corollaries presented in Section 3.2. Similar to the numerical simulation approach in Section 4.3, the varying parameters across the three sensitivity parameter settings are all set to range from  $[-0.16, 0.16]$  with an interval of 0.02.

Figure 8 presents the estimation results as error bar plots for three specific cases of sensitivity parameter values, with confidence intervals derived from 200 bootstrap samples. For Case 1, we find that the sensitivity parameter  $\eta_0$  has a significant impact on the causal relationship from  $X$  to  $Y$ . As  $\eta_0$  increases, the effect gradually weakens, but the causal effect remains positive throughout. Similarly,  $\eta_0$  has a smaller impact on the reverse causal effect from  $Y$  to  $X$ , and this effect also remains positive. For Case 2, we find that the sensitivity parameter  $\delta_0$  has a larger impact on the causal relationship from  $Y$  to  $X$ . As  $\delta_0$  increases, the effect gradually weakens, but it remains positive. In contrast,  $\delta_0$  has a smaller impact on the causal relationship from  $X$  to  $Y$ , and the effect remains positive. For Case 3, the inclusion of two sensitivity parameters affects the causal relationships in both directions. The causal effect of  $X$  on  $Y$  gradually weakens as the sensitivity parameters increase, but remains positive throughout. In contrast, the causal effect of  $Y$  on  $X$  is more substantially influenced and turns negative when the sensitivity parameter exceeds 0.04. Introducing a sensitivity parameter  $\eta_0$  (or  $\delta_0$ ) can be interpreted as adding a causal path, which consequently influences the corresponding causal effect parameter  $\beta_{x \rightarrow y}$  (or  $\beta_{y \rightarrow x}$ ) to some extent.

Overall, whether under the change of  $\eta_0$  or  $\delta_0$ , all bidirectional causal effects exhibit a positive relationship, suggesting that, based on the real-world data, there is a positive causal relationship between "heart disease" and "diabetes", and the sensitivity analysis further validates the robustness of this relationship. Specifically, as the sensitivity parameters change, both the effect of heart disease on diabetes and the reverse effect of diabetes on heart disease maintain a positive direction, indicating a significant bidirectional causal relationship. This relationship remains stable across a range of parameter values, providing reliable evidence supporting the causal relationship between

heart disease and diabetes.

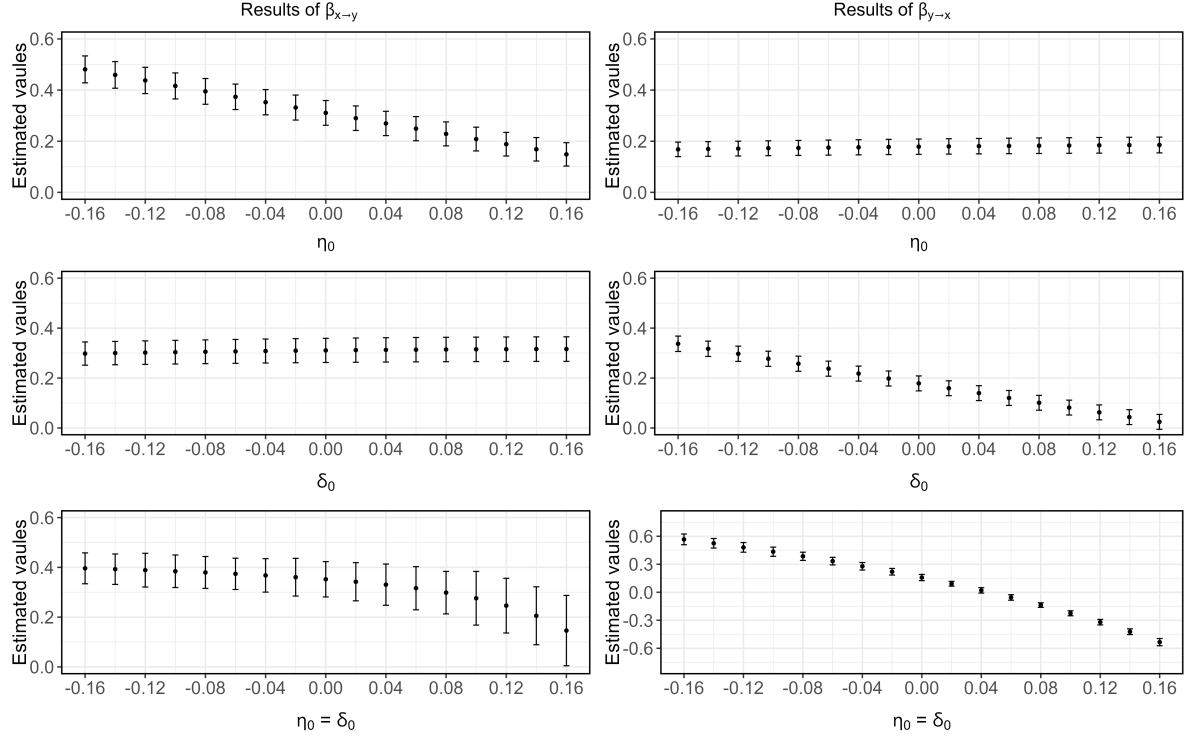


Figure 8: Sensitivity analysis results across three cases for the heart disease and diabetes dataset.

## 6 Summary

This paper develops a framework and method to evaluate bidirectional causal effects between binary variables in the presence of unobserved confounders by mapping continuous latent variables to observed binary outcomes using threshold constraints. To address unobserved confounders in observational studies, we introduce instrumental variables to construct consistent estimators and propose a new identification strategy under the Probit model. Furthermore, we relax the identification assumptions to varying degrees and conduct sensitivity analysis for the proposed method. Finally, we apply the proposed method and corresponding sensitivity analysis to the heart disease dataset to investigate the bidirectional causal relationship between coronary heart disease and diabetes.

There remain several important directions for future research. First, [Clarke and Windmeijer \(2012\)](#) introduced a control function approach for binary outcome variables, achieving identification of unidirectional causal effects in the presence of unobserved confounding. Building on their work, it would be promising to further explore the application of this approach to the identification of bidirectional causal effects. In addition, the method proposed in this paper is designed for binary variables and estimates causal effects based on observed binary data. A natural extension would be to generalize the framework to multi-level settings and consider the use of the ordered Probit model to evaluate bidirectional causal relationships between categorical variables. These extensions

go beyond the scope of this paper and are left for future work.

## Supplementary Materials

The Supplementary Materials contain proofs of the theoretic results and additional simulation studies in the main paper.

## Funding

This work was supported by the National Natural Science Foundation of China (2401378), the Beijing Key Laboratory of Applied Statistics and Digital Regulation, the BTBU Digital Business Platform Project by BMEC, and the Research Foundation for Youth Scholars of Beijing Technology and Business University (RFYS2025).

## Conflict of interest

None declared.

## References

Angrist, J. D., G. W. Imbens, and D. B. Rubin (1996). Identification of causal effects using instrumental variables. *Journal of the American Statistical Association* 91(434), 444–455.

Borracci, T., I. Cappellini, L. Campiglia, F. Piccifuochi, J. Berti, G. Consales, and A. De Gaudio (2013). Preoperative medication with oral morphine sulphate and postoperative pain. *Minerva Anestesiologica* 79, 525–533.

Brownlee, M. (2001). Biochemistry and molecular cell biology of diabetic complications. *Nature* 414, 813–820.

Clarke, P. S. and F. Windmeijer (2012). Instrumental variable estimators for binary outcomes. *Journal of the American Statistical Association* 107(500), 1638–1652.

Cryan, J. F., K. J. O’Riordan, C. S. M. Cowan, K. V. Sandhu, T. F. S. Bastiaanssen, M. Boehme, M. G. Codagnone, S. Cussotto, C. Fulling, A. V. Golubeva, K. E. Guzzetta, M. Jaggar, C. M. Long-Smith, J. M. Lyte, J. A. Martin, A. Molinero-Perez, G. Moloney, E. Morelli, E. Morillas, R. O’Connor, J. S. Cruz-Pereira, V. L. Peterson, K. Rea, N. L. Ritz, E. Sherwin, S. Spichak, E. M. Teichman, M. van de Wouw, A. P. Ventura-Silva, S. E. Wallace-Fitzsimons, N. Hyland, G. Clarke, and T. G. Dinan (2019). The microbiota-gut-brain axis. *Physiological Reviews* 99(4), 1877–2013.

Davey Smith, G. and G. Hemani (2014). Mendelian randomization: Genetic anchors for causal inference in epidemiological studies. *Human Molecular Genetics* 23(R1), R89–R98.

Emerging Risk Factors Collaboration, N. Sarwar, P. Gao, S. R. K. Seshasai, R. Gobin, S. Kaptoge, E. Di Angelantonio, E. Ingelsson, D. A. Lawlor, E. Selvin, M. Stampfer, C. D. A. Stehouwer,

S. Lewington, L. Pennells, A. Thompson, N. Sattar, I. R. White, K. K. Ray, and J. Danesh (2010). Diabetes mellitus, fasting blood glucose concentration, and risk of vascular disease: A collaborative meta-analysis of 102 prospective studies. *The Lancet* 375(9733), 2215–2222.

Engelgau, M. M., P. Zhang, S. Jan, and A. Mahal (2019). Economic dimensions of health inequities: The role of implementation research. *Ethnicity & Disease* 29(Suppl 1), 103–112.

Foster, J. A., L. Rinaman, and J. F. Cryan (2017). Stress & the gut-brain axis: Regulation by the microbiome. *Neurobiology of Stress* 7, 124–136.

Gao, X., L.-X. Meng, K.-L. Ma, et al. (2019). The bidirectional causal relationships of insomnia with five major psychiatric disorders: A mendelian randomization study. *European Psychiatry* 60, 79–85.

Goldberger, A. S. (1972). Structural equation methods in social sciences. *Econometrica* 40, 979–1001.

Hausman, J. A. (1983). Specification and estimation of simultaneous equation models. *Handbook of econometrics* 1, 391–448.

Henning, R. J. (2018). Type-2 diabetes mellitus and cardiovascular disease. *Future Cardiology* 14(6), 491–509.

Katakami, N. (2018). Mechanism of development of atherosclerosis and cardiovascular disease in diabetes mellitus. *Journal of Atherosclerosis and Thrombosis* 25(1), 27–39.

Li, S. and T. Ye (2024). A focusing framework for testing bi-directional causal effects in mendelian randomization. *Journal of the Royal Statistical Society Series B: Statistical Methodology* 00, 1–20.

Lupparelli, M. and A. Mattei (2020). Joint and marginal causal effects for binary non-independent outcomes. *Journal of Multivariate Analysis* 178, 104609.

Palagini, L., C. Baglioni, A. Ciapparelli, A. Gemignani, and D. Riemann (2013). REM sleep dysregulation in depression: State of the art. *Sleep Medicine Reviews* 17(5), 377–390.

Riaz, N., J. J. Havel, V. Makarov, A. Desrichard, W. J. Urba, J. S. Sims, F. S. Hodi, S. Martín-Algarra, R. Mandal, W. H. Sharfman, S. Bhatia, W.-J. Hwu, T. F. Gajewski, C. L. Slingluff, D. Chowell, S. M. Kendall, H. Chang, R. Shah, F. Kuo, L. G. T. Morris, J.-W. Sidhom, J. P. Schneck, C. E. Horak, N. Weinhold, and T. A. Chan (2017). Tumor and microenvironment evolution during immunotherapy with nivolumab. *Cell* 171(4), 934–949.e16.

Smith, J. P. (1999). Healthy bodies and thick wallets: The dual relation between health and economic status. *Journal of Economic Perspectives* 13(2), 145–166.

Ten Have, T. R., M. Joffe, and M. Cary (2003). Causal logistic models for non-compliance under randomized trials with non-compliance and a dichotomous outcome. *Statistics in Medicine* 24, 191–210.

Van der Vaart, A. W. (2000). *Asymptotic Statistics*, Volume 3. Cambridge University Press.

Xie, F., Z. Yao, L. Xie, Y. Zeng, and Z. Geng (2024). Identification and estimation of the bi-directional MR with some invalid instruments. In *Advances in Neural Information Processing Systems (NeurIPS)*, Volume 37, pp. 48256–48291.

Xue, H. and W. Pan (2020). Inferring causal direction between two traits in the presence of horizontal pleiotropy with GWAS summary data. *PLoS Genetics* 16(11), e1009105.

Yin, Y., L. Liu, and Z. Geng (2016). Assessing the treatment effect heterogeneity with a latent variable. *Statistica Sinica* 28(1), 115–135.